

Influence of temperature, stress, and grain size on behavior of nano-polycrystalline niobium

Yu-Ping Yan(晏玉平), Liu-Ting Zhang(张柳亭), Li-Pan zhang(张丽攀), Gang Lu(芦刚), and Zhi-Xin Tu(涂志新)
Citation: Chin. Phys. B, 2024, 33 (**7**): 076201. DOI: 10.1088/1674-1056/ad3b83
Journal homepage: http://cpb.iphy.ac.cn; http://iopscience.iop.org/cpb

What follows is a list of articles you may be interested in

Atomistic evaluation of tension—compression asymmetry in nanoscale body-centered-cubic AlCrFeCoNi high-entropy alloy

Runlong Xing(邢润龙) and Xuepeng Liu(刘雪鹏)
Chin. Phys. B, 2024, 33 (**1**): 016202. DOI: 10.1088/1674-1056/acfc37

Temperature effect on nanotwinned Ni under nanoindentation using molecular dynamic simulation

Xi He(何茜), Ziyi Xu(徐子翼), and Yushan Ni(倪玉山)
Chin. Phys. B, 2024, 33 (**1**): 016201. DOI: 10.1088/1674-1056/acf997

Size effect on transverse free vibrations of ultrafine nanothreads

Zhuoqun Zheng(郑卓群), Han Li(李晗), Zhu Su(宿柱), Nan Ding(丁楠), Xu Xu(徐旭),Haifei Zhan(占海飞), and Lifeng Wang(王立峰)
Chin. Phys. B, 2023, 32 (**9**): 096202. DOI: 10.1088/1674-1056/ace037

Layer thickness dependent plastic deformation mechanism in Ti/TiCu dual-phase nano-laminates

Minrong An(安敏荣), Yuefeng Lei(雷岳峰), Mengjia Su(宿梦嘉), Lanting Liu(刘兰亭), Qiong Deng(邓琼), Haiyang Song(宋海洋), Yu Shang(尚玉), and Chen Wang(王晨)
Chin. Phys. B, 2023, 32 (**6**): 066201. DOI: 10.1088/1674-1056/acb48f

Molecular dynamics simulation of interaction between nanorod and phospholipid molecules bilayer

Xin Wang(王鑫), Xiang-Qin Li(李香琴), Tian-Qing Liu(刘天庆), Li-Dan Zhao(赵丽丹), Ke-Dong Song(宋克东), and Dan Ge(葛丹)
Chin. Phys. B, 2023, 32 (**1**): 016201. DOI: 10.1088/1674-1056/ac6ed8

Influence of temperature, stress, and grain size on behavior of nano-polycrystalline niobium

Yu-Ping Yan(晏玉平), Liu-Ting Zhang(张柳亭), Li-Pan Zhang(张丽攀)†, Gang Lu(芦刚), and Zhi-Xin Tu(涂志新)

School of Acronautical Manufacturing Engineering, Nanchang Hangkong University, Nanchang 330063, *China*

(Received 12 January 2024; revised manuscript received 30 March 2024; accepted manuscript online 7 April 2024)

Atomic simulations are executed to investigate the creep responses of nano-polycrystalline (NC) niobium established by using the Voronoi algorithm. The effects of varying temperature, applied stress, and grain size (GS) on creep properties and mechanisms are investigated. Notably, the occurrence of tertiary creep is exclusively observed under conditions where the applied stress exceeds 4.5 GPa and the temperature is higher than 1100 K. This phenomenon can be attributed to the significant acceleration of grain boundary and lattice diffusion, driven by the elevated temperature and stress levels. It is found that the strain rate increases with both temperature and stress increasing. However, an interesting trend is observed in which the strain rate decreases as the grain size increases. The stress and temperature are crucial parameters governing the creep behavior. As these factors intensify, the creep mechanism undergoes a sequential transformation: initially from lattice diffusion under low stress and temperature conditions to a mixed mode combining grain boundaries (GBs) and lattice diffusion at moderate stress and mid temperature levels, and ultimately leading to the failure of power-law controlled creep behavior, inclusive of grain boundary recrystallization under high stress and temperature conditions. This comprehensive analysis provides in more detail an understanding of the intricate creep behavior of nano-polycrystalline niobium and its dependence on various physical parameters.

Keywords: creep behavior, molecular dynamics simulation, activation energy, stress exponent, nano-polycrystalline niobium

PACS: 62.20.Hg, 87.15.ap, 61.82.Rx **DOI:** 10.1088/1674-1056/ad3b83

1. Introduction

Widely applied nickel-based superalloys can no longer meet the requirements of high-performance aviation engine materials at temperatures above 1200 °C.[1–3] Niobium-based superalloys possess low density and remarkable elevated-temperature properties, which gives them great potential in the applications of aircraft engines.[4–7] Furthermore, niobium acts as an essential alloying element in Zr–niobium alloys widely used in fusion energy, particularly in the field of fission-type space reactors.[8,9] At present, numerous researchers have studied niobium and its alloys through experimental and simulation methods. Tucker *et al.*[10] investigated the mechanical behavior of single-crystal niobium with neutron-irradiated defects and discovered the mechanisms of defect clearing. Jóni *et al.*[11] reported that the dislocation density and grain size significantly affect the strength of polycrystalline niobium. The influence of tilt grain boundaries (GBs) on the tensile properties of niobium was studied through molecular dynamics (MD) simulations.[12]

The creep resistances of crystalline materials are strongly related to the applied stress, ambient temperature, and crystal size. Creep is an influential problem encountered in practical cryogenic applications. The creep properties of materials under different conditions should be carefully examined to predict possible failure. In recent years, numerous studies have concentrated on the creep behaviors of nanocrystalline materials via experimental, computational and theoretical methods.[13–18] The diffusion and grain boundaries of nanopolycrystalline materials are the main factors affecting creep performance and creep mechanisms.[19,20] Van Swygenhoven and Caro[21] discovered that the deformation of grain boundaries is the main mechanism of nickel phase plastic deformation under an extreme stress condition. At elevated temperatures, grain-boundary diffusion dominates over creep behavior, leading the fatigue lifes of numerous materials to decrease.[22] The creep mechanisms, including GB slip, GB diffusion, and dislocation motion, were discussed via molecular dynamics simulations.[23–25] The creep behaviors of nanopolycrystalline materials can be adequately described by the Bird–Dorn–Mukherjee relation,[26] and expressed as follows:

$$\dot{\varepsilon} = \frac{AD_0Gb}{k_BT}\left(\frac{b}{d}\right)^p\left(\frac{\dot{\sigma}}{G}\right)^n \exp\left(-\frac{\Delta Q}{k_BT}\right), \tag{1}$$

where D_0 is the diffusion constant, G is the shear modulus, k_B is the Boltzmann constant, ΔQ is the activation energy, p is the grain size exponent, n is the stress exponent, and T is the temperature. Equation (1) can be used to study the influence of crystal size, temperature, and stress.

Elevated temperature and pressure make the material susceptible to severe creep and erosion, which results in a deterioration of the material's load-bearing strength. It has been confirmed that MD is an efficient technique for understanding the

†Corresponding author. E-mail: yypgoodluck87@163.com

© 2024 Chinese Physical Society and IOP Publishing Ltd

creep characteristics of different compositions.[27] Through the aforementioned study, it becomes evident that niobium-based alloys enjoy widespread utilization. Nevertheless, there is still a gap in analyzing the creep behavior and potential mechanisms of polycrystalline niobium under various creep conditions and grain sizes. The lack of research could potentially hamper the design, preparation, and application of niobium-based alloys. The present study is to investigate into the creep behavior and mechanisms of polycrystalline niobium, by taking into account various grain sizes, different applied stresses, and system temperatures, through molecular dynamics simulations.

2. Computational details

All the simulations were conducted by using LAMMPS software.[28] Three-dimensional nanopolycrystalline cubic BCC niobium structures with dimensions of 20 nm×20 nm×20 nm are created by Voronoi constructions with the help of ATOMSK software.[29] By meticulously managing the number of grains, we have successfully derived polycrystalline niobium models that possess distinct average grain size ranges. Figure 1 shows the initial samples with different grain sizes, where blue and white represent BCC atoms and GB atoms, respectively.

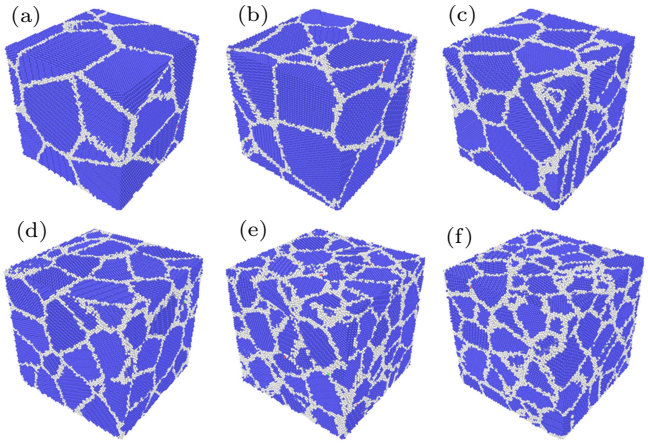


Fig. 1. Microstructures of nanopolycrystalline niobium sample with a size of (a) 11.5 nm, (b) 10.1 nm, (c) 8.5 nm, (d) 7.3 nm, (e) 5.8 nm, and (f) 5.3 nm, respectively.

When completing the establishment of models, the embedded atom method (EAM) potential[30] was utilized to describe the Nb–Nb interactions, which make contribution to the total energy E_i, as described below:

$$E_i = F_\alpha\left(\sum_{j\neq i}\rho_\beta(r_{ij})\right) + \frac{1}{2}\sum_{j\neq i}\phi_{\alpha\beta}(r_{ij}), \tag{2}$$

where F is the embedding energy, ρ is the atomic electron density, and γ is a pair potential interaction.

The periodic boundary conditions (PBCs) are applied to the X, Y, and Z directions. The equations of motion were integrated by employing the Verlet algorithm, with time steps of 1 fs. Then, relaxation processes were conducted for 100 ps in an isothermal–isobar ensemble at a given temperature ranging from 300 K to 1200 K, with an interval of 100 K. As shown in Fig. 1, in the relaxation process and creep process, the system temperature only deviates significantly from the set temperature in the initial stage. However, after a brief period, the system attains a stable condition, and the system temperature remains unchanged in the designated temperature range. By using the Parrinello–Rahman method, different applied stresses ranging from 0.5 GPa to 4.5 GPa with steps of 0.5 GPa, were applied in the X direction (as shown in Fig. 2), while the pressure applied in the other two directions was zero. The timestep of creep deformation was set to 200 ps. The strain can be calculated from the following formula:

$$\varepsilon = (l_x - l_0)/l_0, \tag{3}$$

where l_x denotes the instantaneous length at different timesteps and l_0 is the initial length in the X direction.

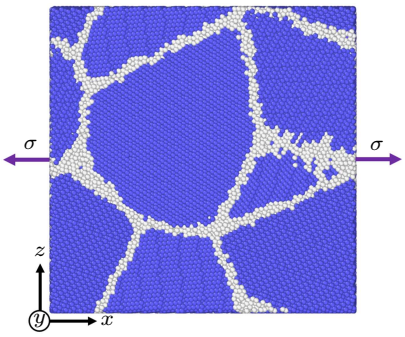


Fig. 2. Schematic diagram of simulated system coordinates and loading method.

The open visualization tool (OVITO)[31] with Wigner–Seitz defect analysis and dislocation extraction algorithm (DXA)[32] were employed for microstructure evolution in creep atomistic processes. Additionally, the atomic diffusion behavior of niobium atoms is explored via the calculation of the mean square distance (MSD). In addition, atomic structures during deformation were investigated via common neighbor analysis (CNA).[32]

3. Results and discussion

3.1. Creep properties of nanopolycrystalline Nb

Temperature is an indispensable factor in creep. Creep simulations were performed on NC Nb with a grain size of 11.5 nm, pressure of 3.0 GPa and various system temperatures. Figure 3 shows the creep strain–time curves of the NC niobium specimens at various temperatures. It can be clearly seen that there is a steady-state creep stage on all the creep curves. At elevated temperatures of 1100 K and 1200 K, a tertiary creep phase can be found in the creep behavior of polycrystalline niobium. This suggests that polycrystalline niobium is more prone to creep failure at elevated temperatures. Both the creep

strain and creep rate increase with temperature rising, and the effect on the latter appears to be more significant. This may be because the higher the temperature, the easier it is for vacancies and atoms to diffuse, accelerating grain boundaries and lattice diffusion.

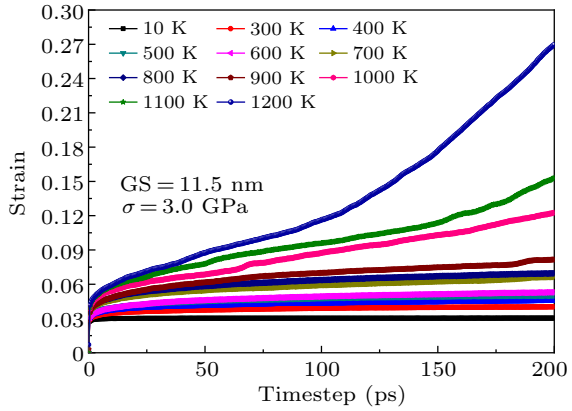


Fig. 3. Strain–time curves for NC niobium at various temperatures.

To explore the influence of applied pressure on the creep properties of NC niobium, the creep behavior was investigated at 300 K and different pressures ranging from 0.5 GPa to 4.5 GPa. Figure 4 shows the creep strain–time curves for distinct applied stresses.

As seen from the curves, the creep rate is susceptible to the applied stress, and the creep strain increases substantially with external stress increasing, especially under extreme stress conditions. When the applied stress reaches 4.5 GPa (60% yield strength, which is obtained through uniaxial tensile simulation), the creep behavior of polycrystalline niobium can manifestly indicate the tertiary creep stage. Moreover, the greater the applied stress, the shorter the secondary creep is. Nonetheless, when the applied pressure is low, the creep behavior of polycrystalline niobium has only two phases within the simulation time range. This may be because higher applied stresses are more likely to overcome the energy barriers of vacancy diffusion, grain boundaries, and dislocation motion.

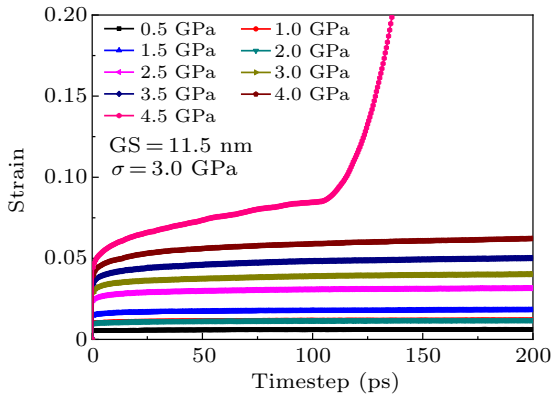


Fig. 4. Strain–time curves for NC niobium under different applied stresses.

Creep simulations of NC Nb with varying grain sizes were performed at 300 K and 3 GPa. Figure 5 shows that the strain increases with grain size decreasing. At a creep time of 200 ps, the strain was 0.04022 for a grain size of 11.5 nm and 0.06223 for a grain size of 5.3 nm, an increase of 55%. The creep rate is lower for larger grain size specimens. The GBs are essential sources and sinks of dislocations and serve as priority channels for atomic diffusion.[33,34] The relationships between yield stress and Young's modulus with grain size in nano-crystalline niobium at 300 K as depicted in Fig. 2, reveals that when the average grain size falls below 11.5 nm, a larger grain size corresponds to superior mechanical properties in nano-polycrystalline niobium. This observation aligns with the inverse Hall–Petch relation. Previous studies have consistently shown that, within the Hall–Petch regime, a decrease in grain size is positively related to the increase of strength and hardness in materials. This is attributed to the increased density of GBs in smaller grains, which effectively hinders dislocation movement and plastic deformation, thereby enhancing the metal's strength. However, it is crucial to note that as the grain size reaches a critical threshold within the inverse Hall–Petch regime, an excessive number of GBs can lead to a preponderance of internal defects and dislocations, ultimately resulting in a decline in tensile properties. This could be attributed to the presence of numerous GBs in the nano-crystalline niobium with minute grain sizes, resulting in an augmentation of grain boundaries and lattice diffusion.

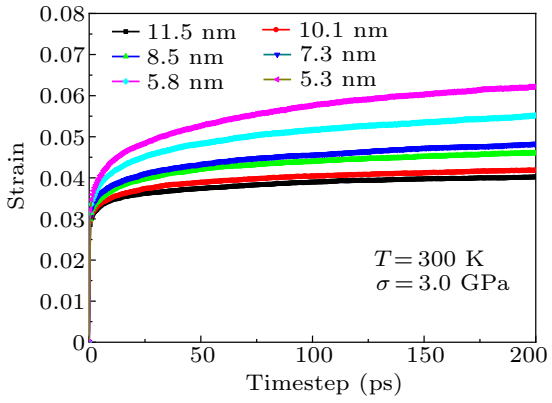


Fig. 5. Strain–time curves of samples with different grain sizes under 3 GPa at 300 K.

3.2. Creep mechanism analysis

We analyze the influence of the applied pressure, ambient temperature, and GS on the creep strain rate to determine the creep mechanism of the NC niobium. The creep rate is calculated from the steady-state creep stage in the strain–time curves. The treated creep deformations are displayed via the OVITO software. The stress index n, creep activation energy ΔQ, and GS exponent p can be calculated from the following equations:

$$\Delta Q = \frac{\partial \ln \dot{\varepsilon}}{\partial (1/k_{\mathrm{B}}T)}, \tag{4}$$

$$n = \frac{\partial \log \dot{\varepsilon}}{\partial \log \sigma}, \tag{5}$$

$$p = \frac{\partial \log \dot{\varepsilon}}{\partial \log d}. \tag{6}$$

Typically, the creep deformation mechanism may be influenced by ΔQ, n, and p. For $n = 1$, the primary creep mechanism is lattice diffusion or GB diffusion.[35,36] For $n = 2$, GB sliding creep can be the staple deformation mechanism.[37] For $n = 3$, dislocation motion may be the dominant creep mechanism.[38]

Figure 6 shows the plots of creep rate *versus* applied stress at diverse temperatures ranging from 0.5 GPa to 4.5 GPa. The variations in the strain rate with stress are the same for different temperatures, while the strain rate noticeably increases when the applied stress varies from low to high. The plot of creep rate versus applied stress can be divided into three stages with turning points of 2.0 GPa and 3.5 GPa and can be fitted linearly separately. As the temperature and stress increase, the stress index n also increases. At a temperature of 300 K, the value of n is approximately 0.73 for stresses below 2.0 GPa, which is referred to as the low stress range (LSR). Within the stress range from 2.0 GPa to 3.5 GPa, known as the medium stress range (MSR), n is approximately 2.56. However, when the stress exceeds 3.5 GPa, entering the high stress range (HSR), n increases significantly to a value greater than 10.55. The stress range is divided into high, medium, and low, the tensile stress–strain curves of niobium samples with varying grain sizes are displayed in Fig. 3 and the creep curves of niobium samples under varying stresses as indicated in Fig. 2. For 600 K, n is approximately 1.03 for LSR, 3.34 for MSR, and 12.81 for HSR. For 900 K, n is about 1.45 for LSR, 3.77 for MSR, and 13.06 for HSR. It is clearly seen that the creep rate is positively influenced by both applied stress and temperature. Temperature exerts a notable influence on the stress index n, with a rise in temperature leading to a corresponding increase in the stress index. In the low stress regime (LSR), the stress index n approximates 1, strongly indicating that lattice diffusion is the primary creep mechanism at play. During the transition to the medium stress regime (MSR), the stress index n lies between 2 and 4, hinting at a combined creep mechanism involving grain boundaries (GBs) and lattice diffusion. However, in the high stress regime (HSR), n attains abnormally high values exceeding 10, suggesting a breakdown of the power-law controlled creep behavior. The magnitude of the stress index serves as a proxy for diverse creep mechanisms. Higher stress contributes to the diffusion of vacancies and nucleation of dislocations in materials, thus accelerating the creep deformation process. Furthermore, grain boundaries function as preferential diffusion paths for vacancies, enabling a higher creep rate under applied stress. Therefore, the creep mechanism of polycrystalline niobium is significantly influenced by the environmental temperature and the external stress.

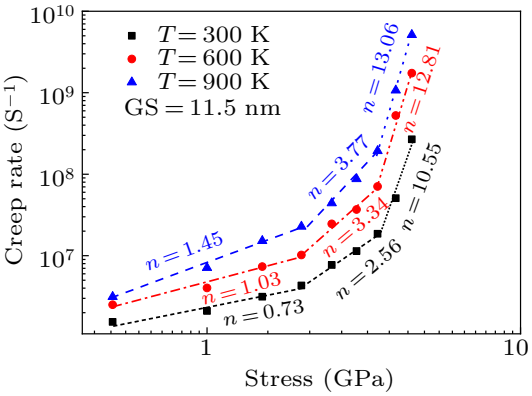


Fig. 6. Double-log plots of the creep rate *versus* applied stress for three different temperatures.

We also explicitly relate the creep rate to the pressure at 900 K for two specimens with different grain sizes and calculate the stress index, as shown in Fig. 7. Studies show that for stresses below 2.0 GPa, the stress index is significantly affected by the GS of the NC Nb. As the pressure increases, the stress indices of the two specimens are significantly different from each other. The relationship between the creep rate and stress can be linearly fitted in two stages for the sample with tiny grains (GS = 8.5 nm), while that of the sample with large grains (GS = 11.5 nm) can be divided into three segments, which proclaims that grain size has a momentous influence on the stress exponent. For the NC niobium sample with a grain size of 11.5 nm, n in the low-stress range (below 2.0 GPa) is 1.65, whereas it is 6.15 in the high-stress zone (exceeding 2.0 GPa). To the best of our knowledge, different n values indicate dissimilar deformation mechanisms.[39,40] It can be inferred that the combined effect of GS and ambient temperature modifies the creep mechanism.

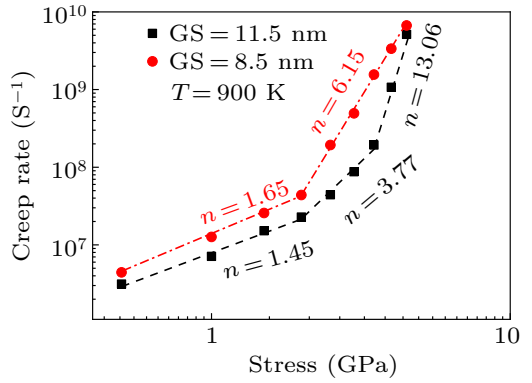


Fig. 7. Double-log plot of the relation between the creep rate and pressure of NC Nb for two different GSs.

We compute the grain size exponent p using Eq. (6) from the creep curves, the results are shown in Fig. 8, which indi-

cates the double-log plots of the creep rate versus GS in different simulation environments. It is obvious that the creep rate declines gradually as the GS increases at various temperatures and stresses. A decrease in the GB volume with GS increasing results in a decrease in the creep rate, which enhances the diffusion of point defects, leading to dislocation emission and absorption. The influence of pressure on the GS index varies depending on elevated temperature environment and low temperature environment. For low temperatures of 300 K, the size parameter increases from 1.657 to 2.649 as the imposed stress increases, suggesting that the greater the stress in the cryogenic environment, the greater the effect of GS on the creep rate is. For the elevated temperatures of 900 K, the size parameter drops sharply from 4.305 to 1.414 with the increase of applied pressure, indicating that GS has a greater effect under the conditions of elevated temperatures and low stress . Therefore, the influence of GS on the creep mechanism is dependent on temperature and stress.

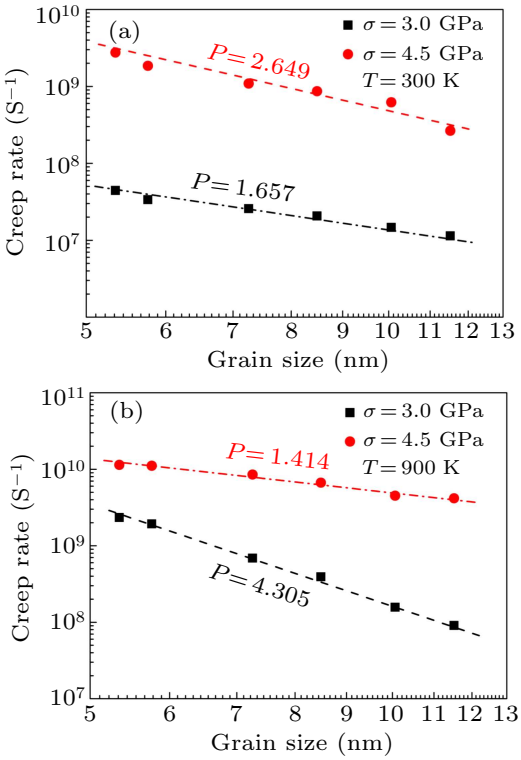


Fig. 8. Double-log plots of creep rate versus GS at two pressure levels and (a) 300 K and (b) 900 K.

The relation between the natural logarithmic creep rate and $1/(k_{\rm B}T)$ is obtained to calculate the creep activation energy ΔQ, which is derived from the Arrhenius equation, as shown in Fig. 9. The slope of each fit line is regarded as ΔQ. Three segments are shown, with 500 K and 900 K as turning points. Previous studies have shown that vacancies remain stationary at up to 700 K and diffuse at 1200 K.[41,42] The creep activation energy ΔQ is 0.0453 eV for low temperature, 0.13 eV for middle temperature and 0.55 eV for high temperature. This may suggest a coupling mechanism involving GB diffusion, atom diffusion and dislocation gliding.

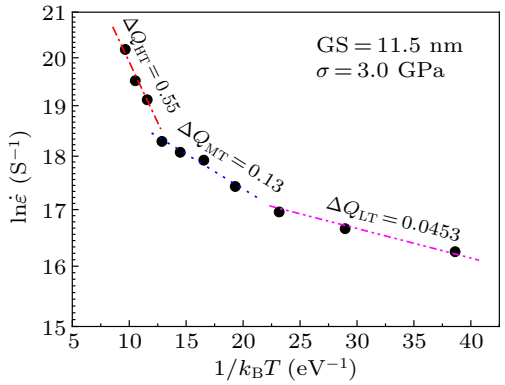


Fig. 9. Plot of ln$\dot{\varepsilon}$ versus $1/(k_{\rm B}T)$ between 300 K and 1200 K.

To study the diffusion mechanisms of nanocrystalline niobium, the mean square displacement (MSD) was also acquired through the following formula:[43,44]

$$\mathrm{MSD} = \sum_{i=1}^{N} \left((r_i(t) - r_i(0) \right)^2, \tag{7}$$

$$\mathrm{MSD} = 6Dt, \tag{8}$$

$$Q_{\rm D} = \frac{\partial \ln D}{\partial \left(\dfrac{1}{k_{\rm B}T} \right)}, \tag{9}$$

where $r_i(0)$ and $r_i(t)$ are the original and current positions of atom i, respectively; D is the diffusion coefficient; $Q_{\rm D}$ is the diffusion activation energy; $k_{\rm B}$ is Boltzmann's constant. We calculated the diffusion coefficient via Eq. (8) from the MSD values. The $Q_{\rm D}$ can be obtained via Eq. (9). Figure 10 shows the plots of MSD versus timestep for NC niobium at different temperatures. The curves show that the MSD per atom increases with time going by and grows steeply with temperature rising. As shown in Fig. 10, at temperatures below 900 K, atomic diffusion is maintained at a stable and relatively low level. The mean square displacement expands significantly with time increasing in the whole creep process when the temperature is above 1000 K.

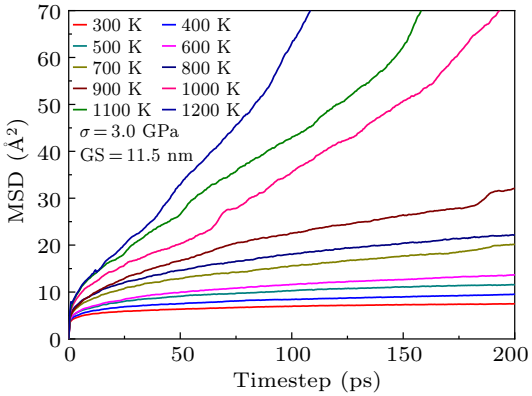


Fig. 10. Plots of MSD versus time at different temperatures for a strain of 11.5 nm under an applied stress of 3.0 GPa.

Figure 11 shows Arrhenius plots of the diffusion coefficient versus $1/(k_{\rm B}T)$ for NC niobium with a GS of 11.5 nm at various temperatures. The diffusion coefficient can be fitted linearly to $1/(k_{\rm B}T)$ in three segments with 500 K and 900 K as turning points. The activation energy values of the diffusive $Q_{\rm D}$ are calculated by using a piecewise linear fit. $Q_{\rm D}$ is 0.0609 eV at low temperature, 0.19 eV at intermediate temperature, and 0.53 eV at elevated temperature, which is equivalent to the creep activation energy ΔQ, as described above. $Q_{\rm D}$ is the summation of the atomic diffusion and the GB diffusion. This may suggest that the creep mechanism can involve the coexistence of dislocation motion, GB diffusion, and lattice diffusion.

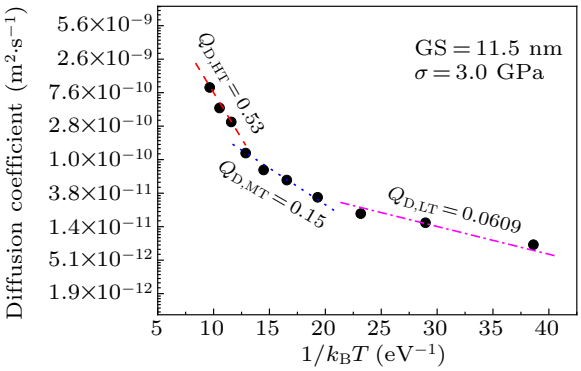


Fig. 11. Arrhenius plot of diffusion coefficient versus $1/(k_{\rm B}T)$ in a temperatures range from 300 K to 1200 K.

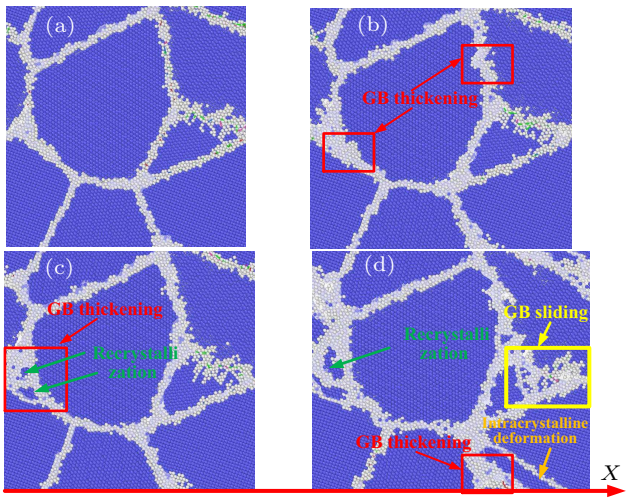


Fig. 12. Cross-sectional snapshots depicting creep process of NC Nb with a grain size of 11.5 nm at 4.5 GPa and 300 K for (a) 0 ps, (b) 10 ps, (c) 50 ps, and (d) 120 ps.

Cross-sectional snapshots depicting the creep process at 300 K under a stress of 4.5 GPa for nanocrystalline niobium with a grain size of 11.5 nm are illustrated in Fig. 12. Figure 12(a) shows the initial configuration of nanopolycrystalline niobium (0 ps), which features grain boundary stacking faults and dislocations. A snapshot of the primary stage (10 ps) is shown in Fig. 12(b), where the sample extends slightly in the X direction. Owing to the diffusion of atoms, grain boundary thickening also occurs distinctly, which is the creep mechanism in polycrystalline materials.[17] Figure 12(c) shows the structure of the sample entering the steady-state creep stage (50 ps). The grain boundaries are obviously elongated and thickened. In this phase, the sliding and diffusion of atoms across the grain boundaries become more intense. Remarkably, recrystallization at large grain boundaries allow disordered atoms to develop into BCC structures. When creep deformation enters the tertiary creep phase, recrystallization and thickening of the grain boundaries become distinct. Moreover, intracrystalline deformation and GB sliding also occur in this process as shown in Fig. 12(d). It can be concluded that atom diffusion, grain boundary thickening and recrystallization are the creep mechanisms at high applied stresses.

DXA atomic snapshots of NC Nb with a GS of 11.5 nm at 300 K under different applied stresses are obtained via OVITO software to explore the effect of stress on deformation, and initial snapshots are used for comparison as shown in Fig. 13. The GBs are not significantly deformed after 100 ps at 1 GPa. The creep mechanism can be lattice-diffusion creep as discussed for the stress index. When the stress is increased to 3 GPa, slight grain boundary slip occurs, but the main deformational behavior is also GB diffusion. Only at pressures up to 4.5 GPa are the pronounced deformations such as grain boundary thickening and sliding with recrystallization observed. We can conclude that high stress can significantly change the creep mechanism.

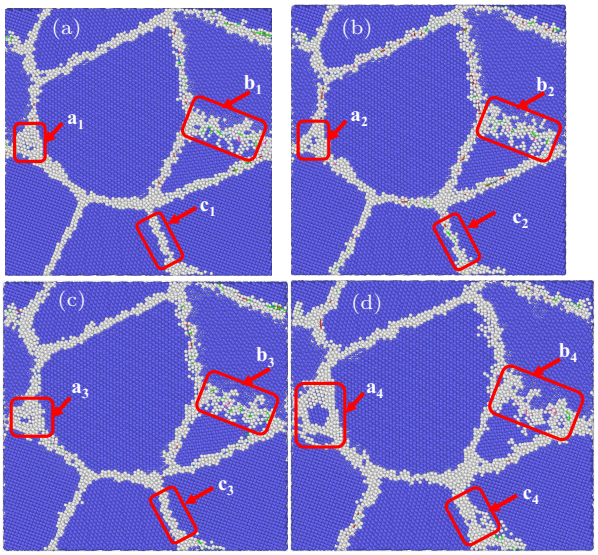


Fig. 13. DXA atomic snapshots of nanocrystalline Nb with a GS of 11.5 nm at 300 K under various pressures: (a) initial(unpressured), (b) 1.0 GPa–100 ps, (c) 3.0 GPa–100 ps, and (d) 4.5 GPa–100 ps.

The effect of temperature on deformation is also tested at moderate stresses. Figures 14(a)–14(d) show the DXA structures of the NC Nb samples for 100 ps at various temperatures under 3.0 GPa. Comparing with the scenario at 300 K,

the sample experiences significant grain boundary coarsening, recrystallization in the GB region (as indicated by the red arrow in the figure), and slight grain boundary sliding at 600 K. For higher temperatures (900 K and 1200 K), the GB thickening, recrystallization in the grain boundaries, GB sliding, and atom diffusion (as indicated by the orange arrow in the figure) become more intense. The higher the temperature, the more intense the atomic diffusion is, with the atomic diffusion significantly stronger at 1200 K than at 900 K as shown in Figs. 13(c) and 13(d). Interestingly, figure 13(e) shows that the total dislocation density of the NC Nb decreases with temperature increasing, while figure 13(f) shows that the proportion of disordered atoms increases with temperature increasing. The higher the temperature, the easier it is for atoms to diffuse, leading to dislocation slip and annihilation, which lowers the total dislocation density and increases the number of disordered atoms. A high temperature facilitates dislocation nucleation and atomic diffusion as a result of a higher creep probability. The increase in temperature leads the creep mechanism to change.

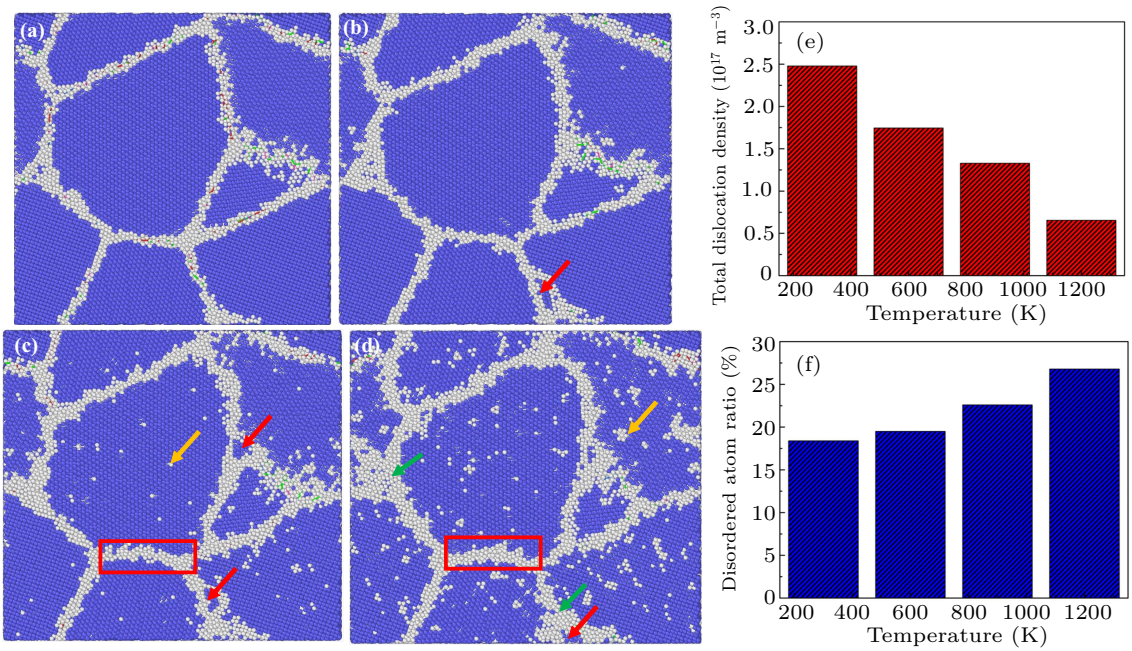


Fig. 14. DXA atomic snapshots of NC Nb with GS of 11.5 nm under 3 GPa at (a) 300 K, (b) 600 K, (c) 900 K, (d) 1200 K, (e) total dislocation density, and (f) disordered atom ratio.

From the aforementioned research, we can draw the conclusion that the applied stress and temperature are pivotal factors influencing the creep mechanism of polycrystalline niobium. As stress levels ascend, the creep mechanism undergoes a transition initially from lattice diffusion to a combination of GBs and lattice diffusion, and ultimately to a disruption of the power-law controlled creep behavior. Notably, the transition thresholds occur approximately at 2 GPa and 3.5 GPa, respectively. Furthermore, within different temperature ranges, the diffusion activation energy and the creep activation energy of polycrystalline niobium are comparable, with higher values observed in the high temperature range. This suggests that the creep deformation of polycrystalline niobium is a composite process encompassing atomic diffusion, grain boundary diffusion, and lattice diffusion.

4. Conclusions

The creep behavior of nano-polycrystalline niobium is thoroughly investigated under varying creep conditions, including different levels of applied stress, temperature, and grain size. The findings can be summarized below.

(i) The tertiary creep is exclusively observable under conditions of pressures exceeding 4.5 GPa and temperatures higher than 1100 K. This can be attributed to the remarkable acceleration of grain boundary and lattice diffusion due to the elevated temperature and stress levels. In addition, a decrease in grain size leads to an increase in creep deformation, primarily due to the increased frequency of grain boundaries, which is conducive to the generation generation and elimination of dislocations.

(ii) The stress index n exhibits different behaviors across three distinct regions, with 2.0 GPa and 3.5 GPa serving as critical thresholds, respectively. As stress increases, the creep mechanism shifts from lattice diffusion to a combined process including grain boundaries and lattice diffusion, ultimately leading to the failure of the power-law controlled creep behavior.

(iii) In different temperature ranges, delineated by the turning points of 500 K and 900 K, the diffusion activation

energy and creep activation energy of polycrystalline niobium exhibit comparable values. The creep phenomena exhibited by nanocrystalline niobium are diverse, encompassing atomic diffusion, grain boundary coarsening, grain boundary diffusion, and dislocation sliding.

(iv) Compared with grain size, temperature and applied stress exert a great profound influence on the creep deformation behavior and underlying mechanisms of polycrystalline niobium.

The insights gained from this study contribute to a profound understanding of the creep behavior of nano-polycrystalline niobium at the atomic level, which may potentially conduce to the design and development of niobium and niobium alloys for various engineering applications.

Data availability statement

The data supporting this paper are available from the corresponding authors upon reasonable request.

Acknowledgement

Project supported by the Doctoral Scientific Research Starting Foundation of Nanchang HangKong University, China (Grant No. EA201903209).

References

[1] Ma J C, Lu Y, Qin Y F, *et al*. 2022 *Appl. Acoust.* **188** 108548
[2] Hachem J, Schuhler T, Orhon D, Cuif-Sjostrand M, Zoughaib A and Moliere M 2022 *Energy* **238** 121656
[3] Xiong B W, Wang C W, Liu K, *et al*. 2020 *Mater. Sci. Eng. A* **799** 140156
[4] Tang Y and Guo X P 2019 *Int. J. Refract. Met. H* **84** 105015
[5] Su L F, Jia L N, Jiang K Y, *et al*. 2017 *Int. J. Refract. Met. H* **69** 131
[6] Sun Z P, Guo X P and Guo B H 2015 *Int. J. Refract. Met. H* **51** 243
[7] Wang N, Jia L N, Kong B, *et al*. 2018 *Int. J. Refract. Met. H* **71** 273
[8] Xiong B W, Wang C W, Xiong Y Z, *et al*. 2019 *Intermetallics* **108** 66
[9] Buckman R W Jr 2004 *Space Tech. Appl.* **699** 815
[10] Tucker R P, Wechsler M S and Ohr S M 1969 *J. Appl. Phys.* **40** 400
[11] Jóni B, Schafler E, Zehetbauer M, *et al*. 2013 *Acta Mater.* **61** 632
[12] Singh D and Parashar A 2017 *Comp. Mater. Sci.* **143** 126
[13] Yang X S, Wang Y J, Zhai H R, *et al*. 2016 *J. Mech. Phys. Solids* **94** 191
[14] Nie K, Wu W P, Zhang X L, *et al*. 2017 *J. Mater. Sci.* **52** 2180
[15] Bhatia M A, Mathaudhu S N and Solanki K N 2015 *Acta Mater.* **99** 382
[16] Millett P C, Desai T, Yamakov V, *et al*. 2008 *Acta Mater.* **56** 3688
[17] Meraj M and Pal S 2015 *Trans. Indian Inst. Met.* **69** 277
[18] Yamakov V, Wolf D, Phillpot S R, *et al*. 2002 *Acta Mater.* **50** 61
[19] Berry J, Rottler J, Sinclair C W, *el al*. 2014 *Phys. Rev. B* **92** 134103
[20] Kasum K, Mulyana F, Zaenudin M, *et al*. 2021 *Jurnal Fisika Flux Jurnal Ilmiah Fisika FMIPA Universitas Lambung Mangkurat* **18** 67
[21] Van Swygenhoven H and Caro A 1997 *Appl. Phys. Lett.* **71** 1652
[22] Zeng, Y P, Li and X Y 2021 *Extreme Mech. Lett.* 44 101253
[23] Wu W P, Chen B, Shen H F and Ding Z J 2022 *Progress in Natural Sciences: International Materials* **32** 259
[24] Jiao S Y and Kulkarni Y 2015 *Comput. Mater. Sci.* **110** 254
[25] Wang Y J, Ishii A and Ogata S 2011 *Phys. Rev. B* **84** 224102
[26] Gowthaman S, Jagadeesha T and Dhinakaran V 2022 *Silicon* **14** 11381
[27] Mchenry M E and Laughlin D E 2000 *Acta Mater.* **48** 223
[28] Plimpton S 1995 *J. Comput. Phys.* **117** 1
[29] Hirel P 2015 *Comput. Phys. Comm.* **197** 212
[30] Tadmor E B, Elliott R S, Sethna J P, Miller R E and Bechker C A 2011 *JOM* **63** 17
[31] Stukowski A 2010 *Mater. Sci. Eng.* **18** 015012
[32] Stukowski A 2012 *Model. Simul. Mater. Sci. Eng.* **20** 045021
[33] Pande C S and Cooper K P 2009 *Prog. Mater. Sci.* **54** 689
[34] Yao H, Ye T Z, Yu W S, Wang P F, Wu J M, Wu Y W and Chen P 2021 *Materials & Design* **206** 109766
[35] Mu J W, Sun S C, Jiang Z H, *et al*. 2013 *Chin. Phys. B* **22** 037303
[36] Coble R L 1963 *J. Appl. Phys.* **34** 1679
[37] Lüthy H, White R A and Sherby O D 1979 *Mater. Sci. Eng.* **39** 211
[38] Weertman J R 1955 *J. Appl. Phys.* **26** 1213
[39] Gowthaman S, Jagadeesha T and Dhinakaran V 2022 *Silicon* **14** 11633
[40] Saha S and Motalab M 2018 *Comp. Mater. Sci.* **149** 360
[41] Aidhy D S, Lu C, Jin K, *et al*. 2015 *Acta Mater.* **99** 69
[42] Xu X, Binkele P, Verestek W, *et al*. 2021 *Molecules* **26** 2606
[43] Ding W Y, He H Y and Pan B C 2015 *J. Mater. Sci.* **50** 5684
[44] Keblinski P, Wolf D and Gleiter H 1998 *Interface Science* **6** 205